electronic reprint

Acta Crystallographica Section B
Structural Science
ISSN 0108-7681

Analysis of $LiKSO_4$ crystals in the temperature range from 573 to 943 K

Carlos Basílio Pinheiro, Marcos Assunção Pimenta, Gervais Chapuis and Nivaldo Lúcio Speziali

Acta Crystallographica Section B
Structural Science
ISSN 0108-7681

Analysis of $LiKSO_4$ crystals in the temperature range from 573 to 943 K

Carlos Basílio Pinheiro,[a]* Marcos Assunção Pimenta,[a] Gervais Chapuis[b] and Nivaldo Lúcio Speziali[a]

[a]Departamento de Física, Icex, Universidade Federal de Minas Gerais, Cep 30123-970, Brazil, and [b]Institut de Cristallographie, Université de Lausanne, BSP, Dorigny CH 1015, Switzerland

Correspondence e-mail: basilio@fisica.ufmg.br

Received 10 November 1999
Accepted 29 February 2000

The structural phases observed in $LiKSO_4$ crystals due to thermotropic transitions have been studied for more than a century. Nowadays many different phases are referenced, but some of the results are still controversial. Structural studies by single-crystal X-ray diffraction from room temperature to 803 K are presented here. Phase II ($708 < T < 943$ K) is extensively discussed on the basis of ordered and disordered models, using harmonic and anharmonic atomic displacements, and considering a twinned crystal composed of three orthorhombic domains. Analyses of the same phase at different temperatures determine the best structure model.

1. Introduction

$LiKSO_4$, lithium potassium sulfate, crystals present a rich sequence of phase transitions over a large temperature range from 30 K up to almost 943 K. The first publication on this compound describes a phase transition at high temperature giving rise to a multi-domain structure (Wyrouboff, 1890); some years later Nacken (1907) determined this transition temperature value as 708 K. Since then a great number of scientific works have been dedicated to this compound using different experimental techniques and varying theoretical approaches. Nevertheless, some of the conclusions stated in the literature are still controversial.

The first structural results of the room-temperature phase (III) were obtained from X-ray powder diffraction (XPD) and the symmetry determined to be $P6_3$ ($Z = 2$; Bradley, 1925). All the atomic positions except those of lithium could be determined. Using single-crystal X-ray diffraction (SCXD) results, Chung & Hahn (1972, 1973) detected a disorder of the anions on the trigonal axis. More recently, Karppinen *et al.* (1983) refined the structure in $P6_3$ ($Z = 2$) assuming that their samples were twinned by L and D domains and using anharmonic vibrations for the O atoms. Bhakay-Tamhane *et al.* (1984) performed neutron diffraction at room temperature and concluded that the structure could be better described using models of disorder. Furthermore, they showed that a refinement on a multi-domain model with $P2_1$ symmetry is numerically equivalent to the refinement in $P6_3$. Using *probability density function* (PDF) analysis at different temperatures in the room-temperature phase, Schulz *et al.* (1985) proposed a structural model consisting of unresolved static disorder superimposed to a significant anharmonic vibration of the O atoms.

Above room temperature $LiKSO_4$ crystals present at least two phase transitions. Using XPD and single-crystal neutron diffraction experiments Li (1984) postulated the existence of a fourfold superstructure ($Z = 8$) above 712 K with symmetry

$P6_3$ and a possible modulated incommensurate phase between 743 and 943 K. In this phase the value of the wavevector **q** would linearly decrease with increasing temperature with $q(823\,\mathrm{K}) = 0.496\,(2)$ and $q(743\,\mathrm{K}) = 0.500\,(2)$. Sankaran *et al.* (1988) analyzed the conclusion obtained by Li (1984) and stated that the experimental results could be interpreted assuming a model of twinned orthorhombic domains with symmetry *Pmcn* or $P2_1cn$ and $Z = 4$. Using XPD Pietraszko (1988) confirmed the symmetry *Pmcn* in the temperature range 743–935 K (phase II), as well as the hexagonal symmetry $P6_3/mmc$ above 935 K (phase I). Ventura *et al.* (1996) found a twinning domain structure between 708 and 943 K by performing SCXD under uniaxial pressure. This work also suggested the possibility of a modulated phase in this temperature range. Scherf *et al.* (1997), using polarization microscopy on thin $LiKSO_4$ single-crystal plates, studied the domain structure growth during the III $\leftrightarrow$ II transition and confirmed the orthorhombic character of phase II. Many publications, *e.g.* Borisov *et al.* (1994) using acoustic wave propagation and Zhang *et al.* (1998) using IR spectroscopy, reported anomalies in their experiments near 740 K. However, only Li (1984) has claimed a symmetry change in the $LiKSO_4$ structure at this temperature.

Considering the most consistent results found in the literature, the phase transition sequence of $LiKSO_4$ can be summarized as indicated in Fig. 1.

In the present work the crystal structure of $LiKSO_4$ in phase II is discussed on the basis of SCXD results. The proposed model consists of three types of orthorhombic domains, oriented at 120° to each other. The possible modulated character of this phase is not taken into account and all the collected intensities are interpreted as main reflections. Models considering structural disorder and including harmonic and anharmonic atomic displacements are discussed.

According to Bachmann & Schulz (1984), Schulz *et al.* (1985) and Kuhs (1988), a differentiation of the static *versus* dynamic character of a disordered crystal (split atomic positions *versus* anharmonicity) can be obtained by comparing, within a single phase, the structural results at different temperatures. Analysis of the Fourier transform of thermal parameters and PDF (probability density functions), and analysis of the average potential energy of an atom in the crystal $\{V(\mathbf{r}) = V_o(\mathbf{r}) - kT\ln[PDF(\mathbf{r})]\}$, termed the *one particle potential* (*OPP*), can reveal the character of the disorder. In order to check the static *versus* dynamical character, data were collected at two temperatures in phase II, 723 and 803 K. In addition, differences between the structure below and above 743 K were sought.

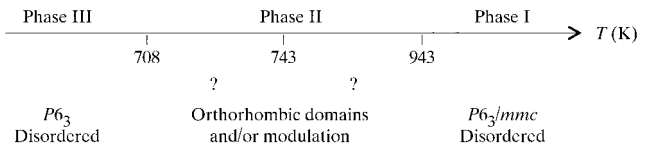

Figure 1
Summary of phase transition sequence in $LiKSO_4$ at high temperatures.

Table 1
Crystal data and data collection parameters in the different measured temperatures.

Crystal data			
Chemical formula	$LiKSO_4$		
M_r (g mol^{-1})	142.1		
Density (Mg m^{-3}) at room temperature	2.328		
Crystal shape, colour	Hexagonal, colourless		
Crystal size (mm)	0.20 × 0.20 × 0.10		
$\mu_{\mathrm{Mo}\ K\alpha}$ (mm^{-1})	1.65 (5)		
Data collection			
λ (Å)	0.71073		
Diffractometer type	Stoe-IPDS®		
Detector type	Image plate		
Detector distance (mm)	50.0		
2θ range (°)	4.6–60.9		
Range of *d(hkl)* (Å)	8.905–0.701		
Scanning type	Oscillations		
Range of φ (°)	30.0–230.0		
$\Delta\varphi$/frame (°)	2.0		
Irradiation time/ frame (min)	9.00		
Measurement temperature (K)	573	723	803
Space group	$P6_3$	*Pmcn*	*Pmcn*
Lattice parameters (Å)	a = 5.202 (1)	a = 5.264 (4)	a = 5.270 (2)
	c = 8.647 (2)	b = 9.148 (2)	b = 9.193 (2)
		c = 8.668 (4)	c = 8.751 (2)
Volume (Å^3)	202.65 (9)	417.7 (3)	424.0 (2)
Range of *hkl*	$-7 \le h \le 7$	$-7 \le h \le 7$	$-7 \le h \le 7$
	$-7 \le k \le 7$	$-12 \le k \le 12$	$-12 \le k \le 12$
	$-12 \le l \le 12$	$-12 \le l \le 12$	$-12 \le l \le 12$
Integrated reflections	2231	13 569	10 251
Unique reflections	396	2380	2401
Observed reflections $[I \ge 3\sigma(I)]$	363	986	807
R_{int}(all)	0.0285	0.0634	0.0815
$R_{\mathrm{int}}[I \ge 3\sigma(I)]$	0.0280	0.0469	0.0519
$R_{\mathrm{e.s.d.}}$(all)	0.0048	0.0235	0.0434
$R_{\mathrm{e.s.d.}}[I \ge 3\sigma(I)]$	0.0051	0.0235	0.0170

2. Experimental

$LiKSO_4$ crystals can present a number of possible merohedral and pseudo-merohedral twins at room temperature (Klapper *et al.*, 1987), some which are not detectable by optical analysis. Suitable samples for the study of phase II were selected through refinements of the room-temperature crystal structure. Only samples with a twin volume ratio close to zero were used. SCXD experiments have been performed using Mo $K\alpha$ radiation. Data were collected at room temperature, 573, 723 and 803 K using hexagonal samples obtained by evaporating a solution containing water and $LiKSO_4$ at 333 K. The diffraction experiments were performed using a Stoe-IPDS® diffractometer equipped with an image-plate detector. The samples were heated by a 2 l min^{-1} dry airflow controlled by an Enraf–Nonius apparatus; the temperature stability was greater than 1 K. Programs of the Stoe-IPDS suite were employed to transform the images into integrated intensities. Lattice parameters were determined using 1668, 1525 and 1469 reflections for the measurements performed at 573, 723 and 803 K, respectively. Table 1 summarizes the data collec-

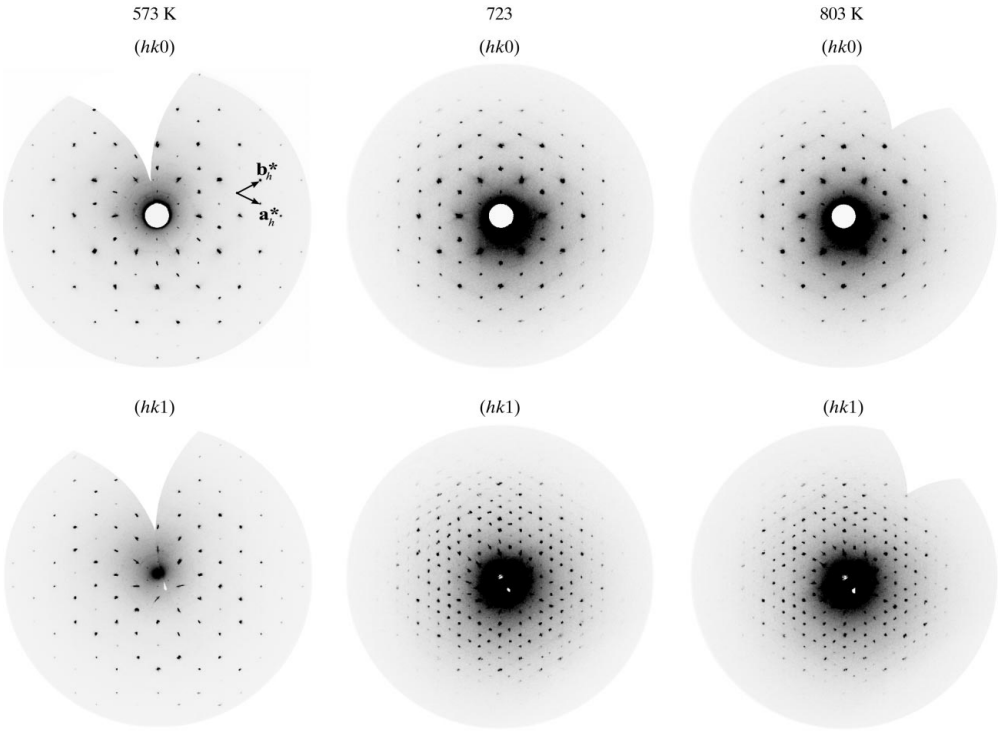

Figure 2
Reciprocal planes (*hk*0) and (*hk*1) in 573, 723 and 803 K. Reconstruction with *SPACE* (Stoe & Cie, 1996).

tion and data reduction parameters for each temperature, as well as the sample characteristics.[1]

The use of the high-temperature apparatus in the Stoe-IPDS® diffractometer caused some geometrical limitations during data collection. As a consequence, the maximum resolution achieved was 0.701 Å ($2\theta_{max} = 60.9°$). The presence of incommensurability in phase II was not investigated. Using the value of $q \simeq 0.49$ mentioned in the literature, the reflection position should be determined with a precision higher than 0.01 in the indices, which was not possible with the image-plate detector. Further data treatment, including structure solution and refinement, was performed using *JANA*98 (Petříček & Dušek, 1998). The function $wR(F)$[2] was refined using full-matrix least-squares.

3. Reciprocal space symmetry

The $LiKSO_4$ reciprocal space was reconstructed using the *SPACE* program (Stoe & Cie, 1996). The transition from phase III to phase II is clearly seen from the analysis of the (*hk*0) and (*hk*1) planes; Fig. 2 shows a representation of these planes. It can be observed that the hexagonal lattice parameters $\mathbf{a}_h^*$ and $\mathbf{b}_h^*$ of the room-temperature phase do not index all the reflections at 723 and 803 K. A refinement of 1281 reflections measured at 723 K in a hexagonal lattice gives $a_h' = 10.530\ (5)$ and $c_h' = 8.684\ (4)$ Å and thus a_h' (723 K) $\simeq 2a_h$ (room temperature). It seems that a similar approach led Li (1984) to propose a superstructure for phase II.

It is worthwhile to point out that no reasonable hexagonal space group is consistent with the observed systematic absences above 708 K; moreover, one must consider the existence of the domain structure as stated by Ventura *et al.* (1996) and Scherf *et al.* (1997). Thus, the $LiKSO_4$ reciprocal space above 708 K can be satisfactorily indexed using the three orthorhombic domains rotated 120° with respect to each other, around the **c** axis. The observed systematic absences are consistent with space groups *Pmcn* or $P2_1cn$. No splitting was observed for any reflection in the experiments using Mo $K\alpha$ and an image-plate detector, indicating a case of twinning by pseudo-merohedry. The broader reflections observed in the diffraction pattern shown in Fig. 2 are consistent with the diffuse scattering discussed by Welberry & Glazer (1994).

4. Crystal structure of phase III

According to Schulz *et al.* (1985), $LiKSO_4$ crystals could be described in space group $P6_3$ with an ordered structure from room temperature to 708 K. However, *PDF* and *OPP* analyses revealed that the O atoms are statically disordered and additionally present strong anharmonic vibrations. The structure should rather be described considering a libration of the O_4 group around the S atom. Above 400 K the lithium atoms also undergo anharmonic vibrations. Karppinen *et al.* (1983), Bhakay-Tamhane *et al.* (1984) and Klapper *et al.* (1987) verified that $LiKSO_4$ samples are frequently naturally twinned comprising two types of domains with a common [110] axis, one being L and the other D. Such a twinning law cannot be identified by optical analysis. Only a complete refinement of the structure can reveal the presence of twinned domains. A set of eight samples has been investigated in the search of a monodomain crystal using the refinement of the domain volume ratio as a guideline. The selected sample presented a ratio of 0.000 (2):1.000 (2) and was used in all the high-temperature SCXD measurements. The results obtained by Schulz *et al.* (1985) have been fully reproduced with a data set collected at 573 K, thus assuring a good sample quality.

The agreement parameters obtained for the adjustment of the 396 unique reflections measured at 573 K are $R = 0.0226$, $wR = 0.0273$ and $S = 2.31$. Refining the 363 observed

[1] Supplementary data for this paper are available from the IUCr electronic archives (Reference: CA0003). Services for accessing these data are described at the back of the journal.
[2] $wR = \sum_j w_j|F_{oj}^2 - F_{cj}^2| / \sum_j F_{oj}^2$; $w = (\sigma^2(F) + 0.0001F^2)^{-1}$.

$[I \geq 3\sigma(I)]$ reflections the agreement parameters are R = 0.0205, wR = 0.0272 and S = 2.42. A total of 40 structural parameters were refined and no significant peaks were found in the final difference-Fourier map. The atomic displacements of the Li and two O atoms were described by third-order tensors in the Gram–Charlier expansion (Willis, 1969; Zucker & Schulz, 1982*a*,*b*; Kuhs, 1988). An **ab** plane projection of the *PDF* map for Li and O1 atoms is shown in Fig. 3. Both atoms present a significant trigonal distortion. The numerical results obtained in the refinements (Table 4) show that U^{11}(O1), U^{22}(O1) and U^{33}(O2) components are larger than the others. This means that the vibration amplitudes are greater in the directions perpendicular to the O—S bond, indicating a significant librational movement of the O4 tetrahedra around the S atom at 573 K. An **ab** projection of the unit cell is shown in Fig. 4. The atomic parameters are listed in Table 4.

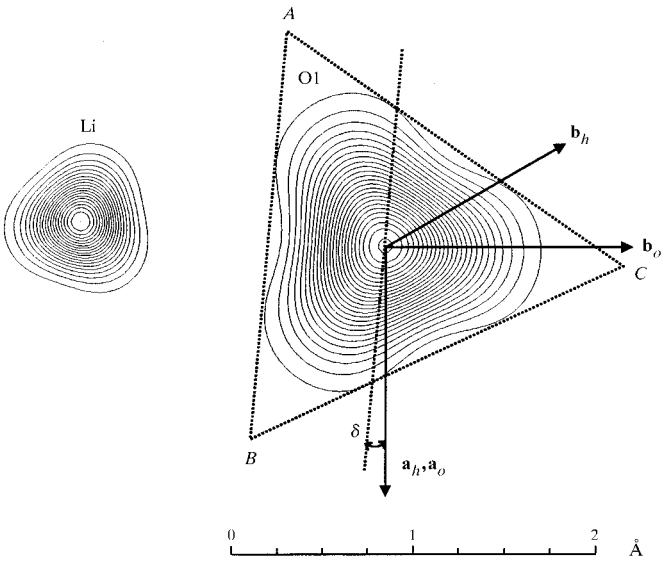

Figure 3
PDF perpendicular to **c** for Li and O1 at 573 K, phase III. The same scale is used for both atoms. *h* and *o* subscripts designate directions in the hexagonal and orthorhombic cells. δ is the angle between the *AB* side of the triangle and a_h

5. Structure determination and refinement of phase II

The resulting domain volume ratio (0:1) in the refinement of phase III guarantees that the studied sample has one unique domain in the room-temperature phase. Therefore, any evidence of twinning above 708 K is a pure consequence of the phase transition III → II. The starting model for the structure solution of phase II considered the crystal as being composed of three orthorhombic domains (Ventura *et al.*, 1996) with symmetry *Pmcn* or $P2_1cn$.

The initial potassium, sulfur and lithium atomic positions in the orthorhombic system were derived from the coordinates of phase III, hexagonal $P6_3$. In *Pmcn* they are on the mirror plane, but on general positions in $P2_1cn$. Difference-Fourier maps calculated with these atoms in both space groups revealed degenerated maxima in the expected oxygen positions, evidencing though a positional disorder for the O_4 group. One example can be seen in Fig. 5. This result suggests using disordered models to refine the structure. The static or dynamic character of the disorder was investigated through the *OPP* analysis of the different O atoms in each temperature studied.

5.1. Models used in the refinement of the structure at 723 and 803 K

The models presented in this section were studied in space groups *Pmcn* and $P2_1cn$ using 1066 and 2130 unique reflections, respectively, for data obtained at 723 K, and 1095 and 2134, respectively, for data obtained at 803 K. Four different models have been considered: an ordered model (ORD), an

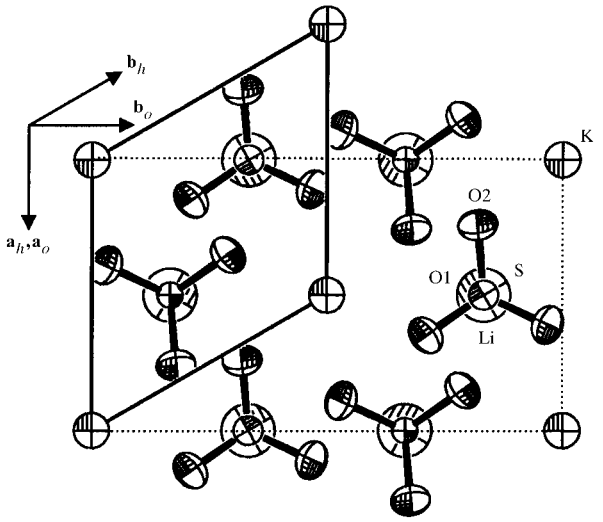

Figure 4
The structure of phase III (573 K) shown in projection onto the **ab** plane. An orthorhombic unit-cell transformation is also represented. Ellipsoids represent 50% probability density.

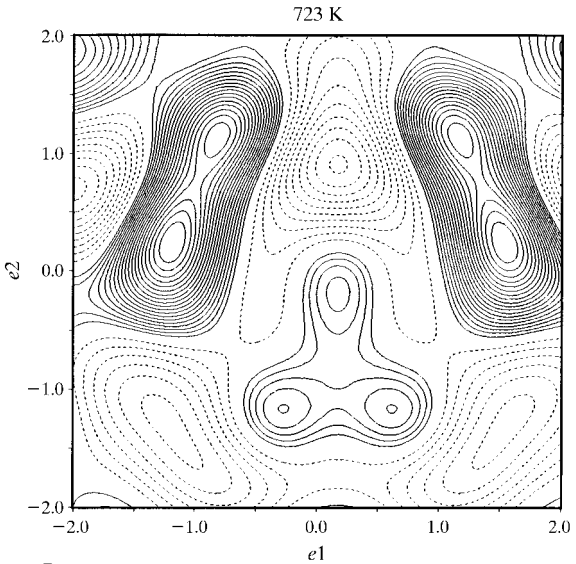

Figure 5
Difference-Fourier map around the S atom in the **c** direction, at 723 K. K, S, Li and O1 atoms contributed to the structure-factor calculation.

Table 2
Results obtained for structure refinements in *Pmcn*.

Use of	*F*
Weighting scheme	$w = 1/[\sigma^2(F) + 0.0001F^2]$
Extinction correction	Not used
Atomic scattering factors	*International Tables for Crystallography* (1992, Vol. C)
Computer programs used	*JANA*98 (Petříček & Dušek, 1998)

	723 K				803 K			
	Ord	Ana	DisA	DisB	Ord	Ana	DisA	DisB
$R(I \geq 3\sigma)$	0.0815	0.0569	0.0643	0.0554	0.0861	0.0709	0.0720	0.0593
$wR(I \geq 3\sigma)$	0.0943	0.0630	0.0751	0.0626	0.0954	0.0753	0.0767	0.0639
$S(I \geq 3\sigma)$	6.04	3.58	4.24	3.55	5.35	4.23	4.34	3.63
R(all)	0.0960	0.0715	0.0795	0.0685	0.1172	0.1044	0.0999	0.0850
wR(all)	0.0947	0.0635	0.0756	0.0630	0.0962	0.0755	0.0775	0.0647
S(all)	5.28	4.09	4.85	4.06	4.35	3.45	3.52	2.95
$(\delta/\sigma)_{max}$	0.0003	0.0001	0.0006	0.00008	0.0004	0.0004	0.0009	0.0004
$\langle(\delta/\sigma)\rangle$	0.0000	0.0000	0.0000	0.0003	0.0000	0.0001	0.0002	0.0000
$\delta\rho_{max}$ (e Å^{-3})	0.53	0.30	0.49	0.32	1.14	1.04	0.86	0.93
$\delta\rho_{min}$ (e Å^{-3})	−0.35	−0.24	−0.31	−0.21	−1.17	−1.01	−1.53	−1.03
Reflections used in refinements (all)	1066	1066	1066	1066	1095	1095	1095	1095
Reflections used in refinements ($I \geq 3\sigma$)	819	819	819	819	726	726	726	726
No. of refined parameters	42	64	54	60	42	64	54	60

ordered model with anharmonic atomic displacements (ANA) and two disordered models A and B (DisA, DisB).

In the ORD model, a unique regular SO_4 tetrahedron was refined; the anisotropic displacement factors were described by second-rank tensors, *i.e.* only harmonic displacements were considered. A second model used in the refinements (ANA) considers an ordered structure in which the vibrations of the O atoms are described by third-order anharmonic tensors in the Gram–Charlier expansion. The same procedure as for phase II (see §4) was used in order to verify whether the conclusions regarding the anharmonic vibrations obtained in the structure analysis of phase III can be extended to phase II. Finally, the last two models aim at testing the possibility of disorder in the SO_4 tetrahedra orientation. A schematic view can be seen in Fig. 6. In model DisA two sets of basal O atoms, light and dark grey, share the common apical oxygen O1, in a special position over m_x, to form two tetrahedra; the disorder consists of a SO_4 rotation around **c**. In model DisB two completely distinct tetrahedra are refined, *i.e.* the four oxygens in the tetrahedron

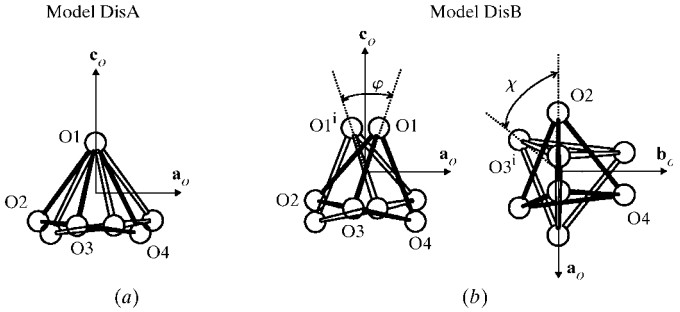

Figure 6
The two disordered models used in the phase II refinements. (*a*) DisA model: two tetrahedra share the apical oxygen O1; (*b*) DisB model: two completely independent tetrahedra related by the m_x symmetry element [(i) $\frac{3}{2} - x, y, z$].

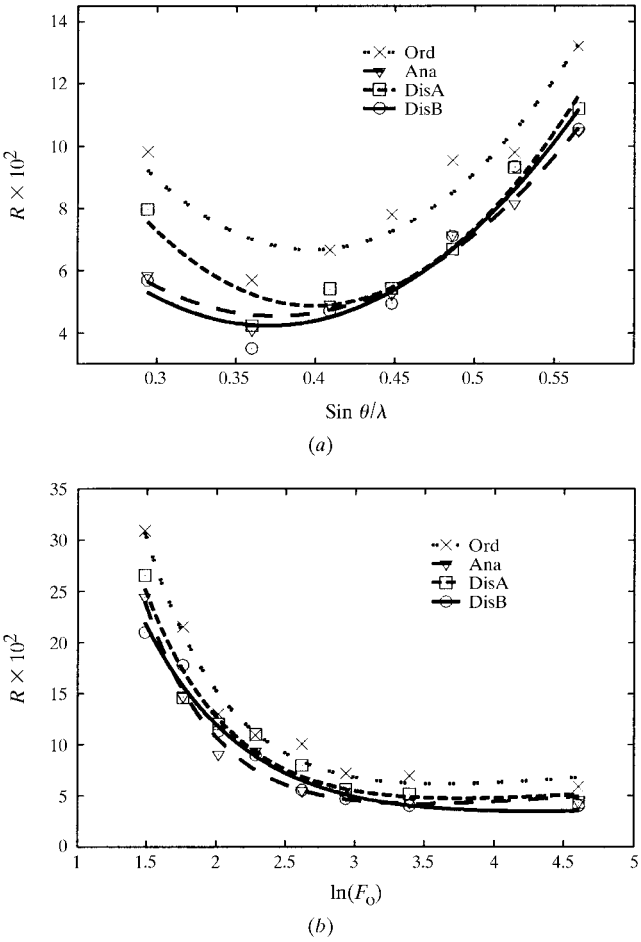

Figure 7
R parameter (*a*) as a function of $\sin\theta/\lambda$ and (*b*) as a function of $\ln(F_o)$ for each investigated model at 723 K. On average, 117 reflections were taken into account for the *R* parameter estimate in each interval.

Table 3
Distances (Å) in 573, 723 and 803 K for each refined model.

The superscripts indicate symmetry elements in each space group. S—O distances were corrected according to rigid-body motion, *i.e.* considering the difference in the U^{ij} components projected along the S—O bond direction.

	Uncorrected Ord				Corrected Ord			
573 K								
S—O1	1.442 (5)				1.48 (1)			
S—O2	1.426 (5)				1.469 (6)			
S—O2^{i}	1.426 (5)				1.470 (6)			
Li—O1	1.99 (2)							
Li—O2^{ii}	1.92 (5)							

Symmetry codes: (i) $1-y, 1+x-y, z$; (ii) $x-y, x, -\frac{1}{2}+z$; in space group $P6_3$.

	Ord	Ana	DisA	DisB	Ord	Ana	DisA	DisB
723 K								
S—O1	1.428 (4)	1.342 (8)	1.424 (4)	1.389 (5)	1.68 (2)	1.56 (2)	1.64 (1)	1.59 (2)
S—O2	1.316 (5)	1.36 (1)	1.435 (7)	1.405 (8)	1.57 (2)	1.66 (4)	1.56 (2)	1.52 (2)
S—O3	1.350 (4)	1.289 (7)	1.33 (2)	1.28 (1)	1.50 (1)	1.47 (2)	1.43 (3)	1.45 (3)
S—O4			1.40 (2)	1.401 (6)			1.57 (4)	1.51 (2)
Li—O1^{i}	1.863 (7)	1.974 (9)	1.913 (6)	1.990 (6)				
Li—O2	1.864 (7)	1.86 (1)						
Li—O2^{ii}			1.94 (1)	1.974 (9)				
Li—O3^{ii}	2.037 (6)	1.995 (8)						
Li—O3^{iii}			2.08 (1)	2.21 (1)				
Li—O4^{iv}			1.93 (2)	1.927 (7)				
803 K								
S—O1	1.454 (7)	1.095 (9)	1.418 (6)	1.415 (7)	1.76 (2)	1.46 (4)	1.67 (2)	1.60 (2)
S—O2	1.322 (5)	1.26 (1)	1.397 (5)	1.354 (9)	1.58 (2)	1.61 (3)	1.56 (2)	1.52 (3)
S—O3	1.333 (5)	1.15 (1)	1.20 (2)	1.24 (2)	1.56 (2)	1.37 (3)	1.49 (8)	1.49 (5)
S—O4			1.38 (2)	1.391 (7)			1.52 (5)	1.51 (2)
Li—O1^{i}	1.904 (9)	2.28 (1)	1.945 (8)	2.069 (7)				
Li—O2	1.867 (8)	1.96 (1)						
Li—O2^{ii}			2.000 (9)	1.99 (1)				
Li—O3^{ii}	2.066 (8)	2.15 (1)						
Li—O3^{iii}			2.24 (2)	2.38 (2)				
Li—O4			1.97 (2)	1.969 (8)				

Symmetry codes: (i) $x, \frac{1}{2}-y, -\frac{1}{2}+z$; (ii) $2-x, -\frac{1}{2}+y, \frac{3}{2}-z$; (iii) $1-x, -\frac{1}{2}+y, \frac{3}{2}-z$; (iv) $\frac{3}{2}-x, y, z$; in space group *Pmcn*.

are split, and even splitting of the S atom was considered; the disorder consists of a rotation of the SO_4 group.

5.2. Refinement analysis

Both space groups *Pmcn* and $P2_1cn$ have been considered in all the proposed refinements. Attempts to refine the extinction parameter did not lead to physically acceptable values (Becker & Coppens, 1974*a*,*b*). Absorption corrections did not change the final results [μ(Mo $K\alpha$) = 1.65 mm^{-1}]. In models DisA and DisB two twin-volume ratio parameters were refined. The agreement parameters are shown in Table 2. Despite the increase in the number of refined parameters for space group $P2_1cn$, the results obtained for *Pmcn* are systematically better in all models. Moreover, it was not possible to separate the non-centrosymmetric sub-domains in the original set of data and therefore not possible to calculate the Flack parameter (Flack, 1983). As a consequence, only the results obtained for *Pmcn* will be considered in the following discussions, assuming the higher symmetry for the crystal structure description.

The quality in the fitting of the different models can be considered by analysing the values of R for data obtained at 723 K as a function of $\sin\theta/\lambda$ and $\ln(F_o)$. In Figs. 7(*a*) and (*b*) it can be seen that the ORD model presents the higher R value in the entire measured range. The strong reflections are almost

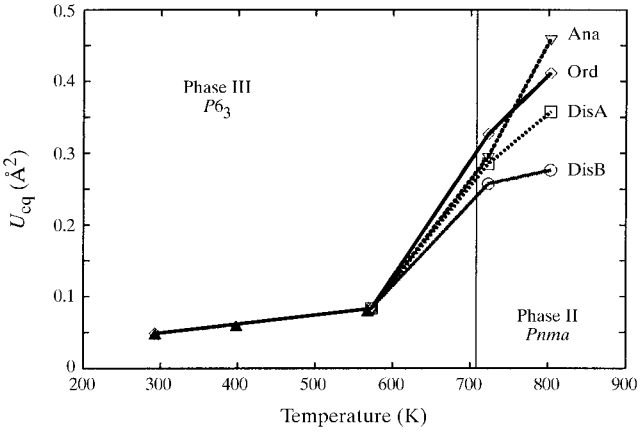

Figure 8
U_{eq}(O1) as a function of temperature. Full triangles are from Schulz *et al.* (1985).

Table 4
Atomic parameters refined in the space group *Pmcn* at 723 and 803 K.

x, *y* and *z* represent fractional coordinates, while U^{ij} and U_{eq} are given in Å^2. *M*: multiplicity; *a*: occupation; $U_{eq} = (U^{11} + U^{22} + U^{33})/3$.

Model		*M*	*a*	*x*	*y*	*z*
Phase III	K	3	1	0	0	0
$P6_3$	Li	3	1	1/3	2/3	0.311 (2)
T = 573 K	S	3		1/3	2/3	0.70785 (9)
	O1	3	1	1/3	2/3	0.5408 (8)
	O2	1	1	0.3590 (7)	0.4211 (6)	0.7617 (6)
Phase II	K	2	1	0.2	0.2050 (1)	0.99706 (8)
Pmcn	Li	2	1	0.75	0.0779 (4)	0.6603 (5)
DisB	S	2	1	0.7500 (7)	0.4048 (1)	0.78394 (9)
T = 723 K	O1	1	0.5	0.670 (2)	0.400 (1)	0.9370 (5)
	O2	1	0.5	1.000 (1)	0.442 (1)	0.7481 (8)
	O3	1	0.5	0.598 (2)	0.498 (1)	0.723 (2)
	O4	1	0.5	0.842 (1)	0.2692 (6)	0.7347 (7)
Phase II	K	2	1	0.25	0.2070 (1)	0.9972 (1)
Pmcn	Li	2	1	0.75	0.0776 (5)	0.6599 (5)
DisB	S	2	1	0.7500 (9)	0.4059 (2)	0.7809 (1)
T = 803 K	O1	1	0.5	0.655 (2)	0.401 (1)	0.9316 (6)
	O2	1	0.5	0.994 (2)	0.443 (1)	0.7488 (9)
	O3	1	0.5	0.612 (3)	0.489 (2)	0.707 (2)
	O4	1	0.5	0.847 (2)	0.2717 (7)	0.7350 (9)

Model		U^{11}	U^{22}	U^{33}	U^{12}	U^{13}	U^{23}	U^{eq}
Phase III	K	0.0484 (2)	0.0484 (2)	0.0443 (3)	0.0242 (1)	0	0	0.0471 (2)
$P6_3$	Li	0.034 (1)	0.034 (1)	0.052 (4)	0.0170 (6)	0	0	0.040 (1)
T = 573 K	S	0.0255 (2)	0.0255 (2)	0.0265 (2)	0.0127 (1)	0	0	0.0258 (2)
	O1	0.111 (2)	0.111 (2)	0.0303 (8)	0.0557 (8)	0	0	0.084 (1)
	O2	0.0588 (8)	0.0450 (7)	0.0981 (9)	0.0329 (6)	−0.0019 (8)	0.0186 (8)	0.0642 (6)
Phase II	K	0.1066 (7)	0.1157 (6)	0.0895 (5)	0	0	0.0054 (4)	0.1039 (3)
Pmcn	Li	0.059 (2)	0.067 (3)	0.090 (3)	0	0	0.002 (2)	0.072 (1)
DisB	S	0.0751 (8)	0.0800 (8)	0.0747 (5)	0.034 (2)	0.019 (2)	0.0025 (6)	0.0766 (4)
T = 723 K	O1	0.27 (1)	0.45 (1)	0.092 (2)	−0.162 (8)	0.098 (5)	−0.049 (4)	0.273 (5)
	O2	0.022 (3)	0.235 (8)	0.236 (7)	−0.031 (3)	0.023 (2)	−0.080 (5)	0.165 (3)
	O3	0.120 (6)	0.280 (9)	0.44 (2)	−0.011 (6)	−0.019 (7)	0.26 (1)	0.281 (7)
	O4	0.133 (6)	0.103 (3)	0.32 (1)	−0.006 (3)	0.018 (3)	−0.084 (4)	0.187 (5)
Phase II	K	0.1236 (9)	0.1365 (9)	0.1027 (6)	0	0	0.0052 (6)	0.1209 (5)
Pmcn	Li	0.067 (3)	0.059 (3)	0.083 (3)	0	0	0.008 (3)	0.069 (2)
DisB	S	0.078 (1)	0.089 (1)	0.0864 (7)	0.036 (2)	0.019 (2)	0.0049 (8)	0.0845 (5)
T = 803 K	O1	0.25 (1)	0.48 (1)	0.106 (3)	−0.151 (9)	0.088 (5)	−0.055 (6)	0.276 (6)
	O2	0.018 (3)	0.28 (1)	0.285 (9)	−0.054 (4)	0.027 (3)	−0.077 (7)	0.196 (5)
	O3	0.16 (1)	0.40 (2)	0.63 (3)	−0.059 (8)	−0.06 (1)	0.41 (2)	0.40 (1)
	O4	0.152 (7)	0.090 (4)	0.37 (2)	0.007 (3)	0.038 (5)	−0.074 (4)	0.204 (6)

equally adjusted in all the models, while for the weak and low-angle reflections, DisB and ANA models give remarkably lower *R* values. It can be concluded that the global results listed in Table 2 are not biased.

The twin volume ratio *V*1:*V*2:*V*3 is essentially the same in the three models [0.629 (8):0.094 (2):0.277 (5) for 723 K and 0.63 (1):0.088 (3):0.288 (6) for 803 K]. According to Ventura *et al.* (1996), a uniaxial pressure can induce domain reductions in the crystal depending on the force direction. In the sample preparation for the X-ray diffraction experiments the single crystal was fixed to a glass fiber with organic cement, which might have interfered in the original twin growth ratio. Thus, the *V*1:*V*2:*V*3 values contain characteristics of the experiment and do not necessarily express the intrinsic twin volume ratios.

The oxygen U^{ij} values obtained in phase II are generally high, but this is also observed in the results obtained for similar compounds at similar temperatures ($RbLiSO_4$: Steurer *et al.*, 1986; Na_2SO_4: Naruse *et al.*, 1987; Na_2SO_4: Tanaka *et al.*, 1991). Refinements in space group $P2_1cn$ did not improve these values. It might be emphasized that large anisotropic displacement components for the O atoms were observed by Zhang *et al.* (1988) for $LiKSO_4$ crystals even at 200 K. This means that the effective potential for the O atoms is large in a wide temperature range, thus contributing to the enlargement of the thermal amplitudes. Taking into account that the components of the anisotropic displacement parameters of oxygen perpendicular to the S—O bonds are greater than along the bond as observed in phase III, the large oxygen U^{ij} can be associated with a rigid libration of the O atoms around

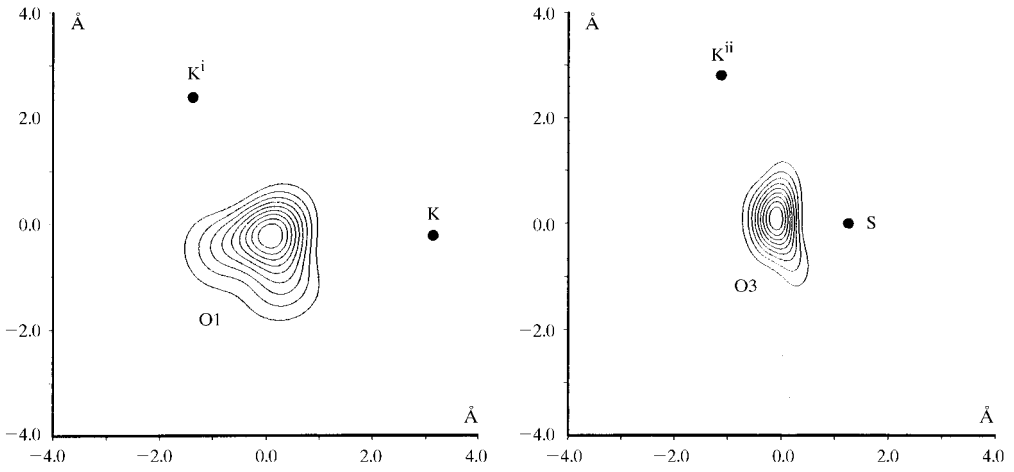

Figure 9
(*a*) *PDF* values for O1 in the K—O1—K^{i} plane and (*b*) for O3 in the K^{ii}—O3—S plane. Symmetry codes: (i) $1+x, y, z$; (ii) $1+x, \frac{1}{2}-y, -\frac{1}{2}+z$.

Oxygen *PDF* maps are drawn in Fig. 9. It can be easily seen that bond constraints in the O atoms lead to small displacements in the O—K and O—S bond directions. The libration of the O atoms is evidenced by the spreading of the density in a direction almost perpendicular to O—S. In the ANA model, the maximum *PDF* (minimum *OPP*) for the O atoms does not coincide with the refined atomic positions. The calculated *OPP* for the O1 atom is plotted in Fig. 10. The abscissa indicates the variation between the refined O1 position and the position of the *OPP* minimum. This corresponds to distinct directions for each temperature. At 723 and 803 K the maximum *PDF* position is 0.17 (1) and 0.32 (1) Å, respectively, away from the refined O1 coordinates, and 1.4864 (7) and 1.418 (1) Å, respectively, from the S atom. For phase III, Schulz *et al.* (1985) interpreted similar results as a consequence of a static disorder with unsplit atoms.

the sulfur. The smaller experimental resolution achieved in phase III does not allow a discussion concerning thermal parameters for the lithium as it was performed in phase II.

The interatomic S—O distances calculated from the refined atomic positions are systematically smaller than the expected values. However, the correction for libration[3] $d_c = d(1+l)$ (Johnson, 1969/1970; Schefer *et al.*, 1998) in the DisB model leads to acceptable results (Table 3).

Careful analysis of the oxygen thermal parameters shows a distinct evolution for the U^{ii} components in each refined model. In general, the DisB model presents the smallest values for the U^{ii} components perpendicular to the S—O bond at both temperatures. The U_{eq} values for the O1 atom obtained for each model are represented in Fig. 8. The solid triangles correspond to the values obtained by Schulz *et al.* (1985) in phase III, which are similar to the results obtained in the present work (the 293 K structure refinements are not discussed here). As a consequence of the large discontinuity in the U_{eq} values owing to the phase transition, a linear extrapolation to 0 K cannot be used to distinguish the static *versus* dynamical character of the disorder as proposed by Schulz *et al.* (1985). Such an extrapolation gives negative values for all the models, except DisB for which U_{eq} (T = 0 K) = 0.0167 Å^2.

The libration amplitude calculated for the O1 atom shows an abrupt variation at the III $\leftrightarrow$ II transition. In each range of investigated temperatures the changes in the libration amplitude (Δl) are much smaller than at the transition. The variation of Δl between 273 and 573 K and between 723 and 803 K is $\sim 2^\circ$. In the transition temperature range between 573 and 723 K, $\Delta l \simeq 13^\circ$. The phase transition is thus clearly characterized by a jump in the SO_4 group libration, and thus restrains in the Li—O bonds are relaxed during the phase transition.

Based on the numerical results of the refinements (*R*, *wR*, *S etc.*), the process of mapping atomic electron density using anharmonic thermal tensors or using split atomic positions are equivalent. Therefore, the agreement parameters of the crystallographic refinements cannot be used as a unique indicator to choose the best model. According to Bachmann & Schulz (1984) and Kuhs (1988), an indirect way to distinguish between split static disorder and anharmonicity is to determine the dependence of the *OPP* on temperature: a temperature-dependent potential indicates the existence of static disorder. Fig. 11 shows the *OPP* in the Oj—K^{i} bond directions (i and j run over different atoms). The potential was calculated using the anisotropic displacement parameters refined in the ANA model. It can be seen that the oxygen *OPP* is qualitatively different at different temperatures within the same structural phase, corroborating the existence of static disorder. With this additional result it can be concluded that the $LiKSO_4$ structure in phase II presents static (or split) disorder.

6. Discussion

Considering the agreement parameters obtained in the structural refinements, the corrected S—O distances in the SO_4 group, the behavior of the anisotropic displacement parameters and consequently the behavior of the libration and the effective *OPP* for the O atoms, it can be concluded that the DisB model best describes phase II. Atomic parameters of the DisB model at 723 and 803 K are listed in Table 4.

[3] The libration amplitude l in radians is equal to $(U_\perp - U_{||})^{1/2}/d^2$, where d is the distance without correction, $U_\perp$ is the component of U(O) perpendicular to S—O and $U_{||}$ is the component of U(O) parallel to S—O.

In order to analyse the structural differences between phase III (573 K) and phase II (723 K), different projections of the $LiKSO_4$ unit cell are shown in Fig. 12. The hexagonal axes of phase III were transformed to the orthorhombic axes of phase II ($\mathbf{a}_o = 2\mathbf{b}_h + \mathbf{a}_h$; $\mathbf{b}_o = \mathbf{b}_h$;$\mathbf{c}_o = \mathbf{c}_h$). The lattice parameters were rescaled and a common origin on the K atom was chosen, thus only one potassium (K_{III} in 573 K and K_{II} in 723 K) presents a relative displacement during the transition. These changes allow a direct comparison of the relative atomic positions. In the **bc** plane projections it can be easily seen that two of the SO_4 groups invert the orientation of the apical oxygen relative to **c** from phase III to phase II. As a consequence, remarkable movement of the K, S and Li atoms occurs. The distance between K_{III} and K_{II} is 0.825 Å, between Li_{III} and Li_{II} 1.331 Å and between S_{III} and S_{II} 0.860 Å.

The **ab** projections in Fig. 12 show that in each unit cell of $LiKSO_4$ in *Pmcn* symmetry only the SO_4 groups near $(\frac{1}{2}, y, z)$ and $(\frac{1}{2}, y, z + \frac{1}{2})$, which are second neighbors in different basal planes, invert the orientation when compared with phase III. Of course, owing to the $P6_3$ symmetry, two equivalent sets of SO_4 groups induce a threefold degeneracy, which leads to the observed threefold twinning.

Considering the physical properties and symmetry changes, the III $\leftrightarrow$ II transition in $LiKSO_4$ can be considered as a reconstructive phase transition. In a theoretical study on A_2XO_4 compounds, Luk'yanchuk *et al.* (1998) proposed that the orientation of the XO_4 groups is determined by dipolar interactions between the first neighbors in the same basal plane, and the first and second neighbors of the nearest basal planes. Their results indicated antiferro-like interactions between the first XO_4 neighbors in the plane and an angular dependency with $\theta = \text{arctg}(c/3^{1/2}a)$ for the character ferro/antiferro for the interaction of the out-of-plane neighbors. A simplified calculation performed using only two tetrahedra groups showed that the interaction is antiferro if $c/a < 1.63$ and ferro if $c/a > 1.63$. In $LiKSO_4$ the c/a ratio decreases monotonically from 1.679 at 290 K to 1.648 at 723 K, *i.e.* ~ 1.65 at the transition point. These results show quite a good agreement between theory and experiment.

Observing Fig. 12 it can be seen that in the phase III $\rightarrow$ phase II transition the Li atoms move in a direction almost parallel to **c** and that the two SO_4 groups rotate around an axis approximately parallel to **a** (**c** and **a** directions are common to both phases). The rotation direction was determined after Fig. 3, where the δ angle (-4.5°) is the deviation in the orientation of the trigonal oxygen atom (O1) from the hexagonal basal axis. It can be shown that a rotation of 69.8°, in addition to a reflection m_x intersecting the ordered SO_4 group, reproduces the structure of the disordered phase II (Fig. 13). In this rotation the basal oxygen $O2^2$ of phase III is transformed in the apical oxygen of phase II.

The analysis of the structural results of phase II is facilitated by decomposing the disorder in the SO_4 groups in two types of displacements, as indicated in Fig. 6(*b*). A tilt is associated with the angle φ between O1—S—$O1^i$ [(i) $\frac{3}{2} - x, y, z$]. It shows the deviation of the apical oxygen from the **c** axis. A twist described by the rotation χ of the tetrahedra around an axis parallel to the O1—S (or the equivalent $O1^i$—S) direction can be measured by the angles between O4—S—$O4^i$ or O2—S—$O3^i$. The distances between the O atoms and/or the values of φ and χ are temperature dependent. Table 5 presents a selection of the calculated distances and angles at 723 and 803 K and a linear extrapolation of these values to 943 K (phase II $\leftrightarrow$ I transition temperature).

The high-temperature structure (phase I) is usually described in space group $P6_3/mmc$, isomorphic to α-K_2SO_4, in a disordered model in which the SO_4 groups are statistically oriented up and down with respect to **c**. As previously mentioned, $\varphi \simeq 70^\circ$ would be sufficient to cause an inversion of

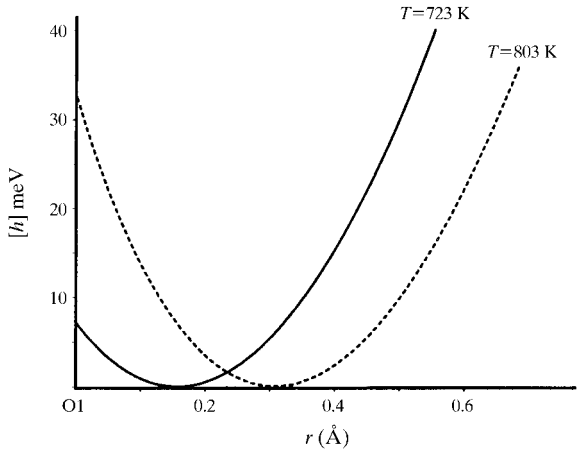

Figure 10
OPP for O1 in the link direction O1–minimal of the potential. Directions are distinct for each temperature: **r** = (0.0117**b** − 0.0142**c**) at 723 K; **r** = (0.0068**b** − 0.0356**c**) at 803 K.

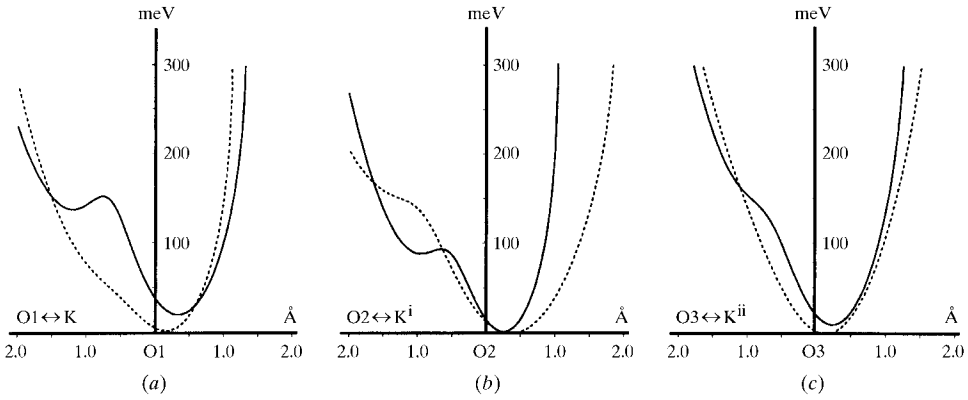

Figure 11
OPP around the O atoms at 723 (dashed lines) and 803 K. (*a*) O1—K direction, (*b*) O2—K^i direction and (*c*) O3—K^{ii} direction. Symmetry codes: (i) $x, \frac{1}{2} - y, -\frac{1}{2} + z$; (ii) $1 + x, \frac{1}{2} - y, -\frac{1}{2} + z$.

the SO_4 unit in relation to **c**, allowing one of the Oj (j = 2, 3 or 4) atoms to occupy the O1 apical position in the tetrahedra. In Table 5 the values extrapolated to 943 K are smaller than 70°. However, transition phase II ↔ I is of a second-order type (without discontinuity) and it can be concluded that from 803 to 943 K a non-linear variation of the χ angle occurs. This hypothesis is corroborated by a number of experiments where physical properties behave in a similar way: *e.g.* Pietraszko (1988) by studying thermal expansion coefficients and Pimenta *et al.* (1989) by studying electrical conductivity.

During the III → II phase transition the SO_4 tetrahedra rotates around an axis almost parallel to $\mathbf{a}_h$ (or $\mathbf{a}_o$). In phase II the φ angle characterizes a rotation of the SO_4 group around the $\mathbf{b}_o$ axis, which increases with temperature. This indicates that the dynamical behavior of the SO_4 group is different during the III ↔ II and II ↔ I phase transitions.

7. Conclusions

In the present work the existence of modulation in phase II of $LiKSO_4$ crystals was not considered owing to the limitation of the experimental resolution. Possible satellite reflections ($q \simeq 0.49$) were included as the main reflections in the structure refinements. According to the present analysis, phase II consists of three types of orthorhombic twinned domains, with *Pmcn* symmetry, oriented at 120° to each other. Attempts to refine the structure using ordered models gave unsatisfactory results. Disordered models based on anharmonic thermal vibrations (ANA) and split atomic positions (DisB) converged to similar numerical results. The *OPP* curves obtained from thermal anharmonic parameters for the O atoms are temperature dependent, indicating that the disorder has a static character and that it is not only a numerical artefact used to describe molecules moving with large libration amplitudes. The static disorder in phase II of $LiKSO_4$ must be understood as a low-frequency ($\ll 10^{18}$ Hz) hopping of atoms between the two sites.

By analysing the agreement parameters, the difference-Fourier maps, the thermal evolution of anisotropic displacements and considering mainly the conclusions based on the *OPP* results, model DisB best describes the structure of phase II. In this phase, the superposition of the *PDF* maps for O1 and O1^{i} [(i) $\frac{3}{2} - x, y, z$] obtained using the DisB model has a similar shape to that observed in the *PDF* map in phase III

Table 5
Distances (Å) and angles (°) quantifying the disorder degree in $LiKSO_4$ at 723, 803 and 943 K.

The 943 K values are obtained from a linear extrapolation of the parameters refined in the DisB model.

	723 K	803 K	943 K
O1—O1^{i}	0.83 (1)	1.0 (1)	1.30
O2—O3^{i}	0.76 (1)	0.79 (2)	0.82
O4—O4^{i}	0.97 (1)	1.02 (1)	1.11
φ (O1—S—O1^{i})	35.1 (5)	41.1 (5)	51.6
χ (O2—S—O3^{i})	32.3 (6)	35.2 (8)	40.3
χ (O4—S—O4^{i})	40.4 (4)	42.9 (5)	47.3

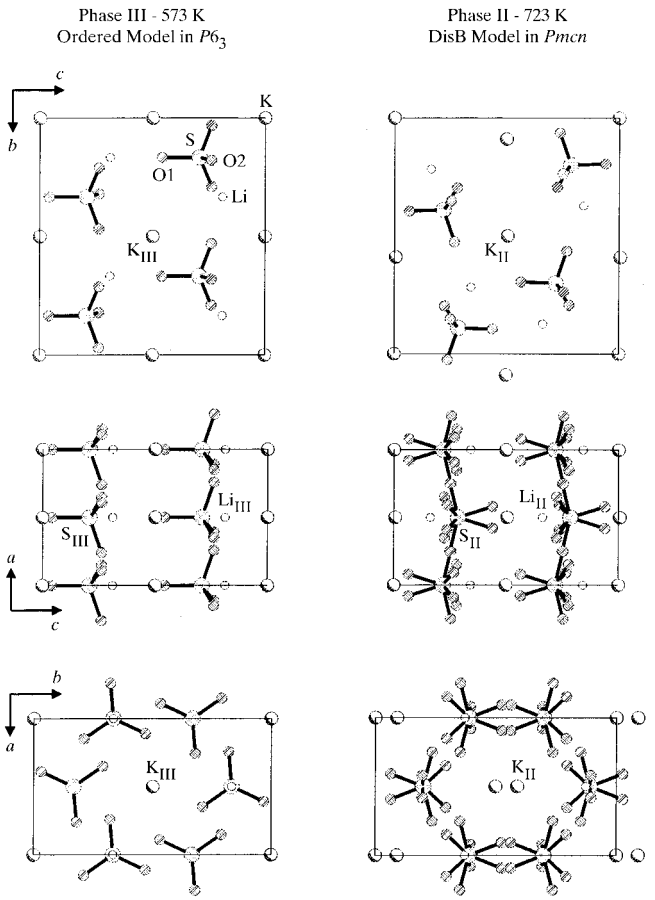

Figure 12
$LiKSO_4$ projection along lattice basis vectors. For the sake of comparison the hexagonal structures (phase III) are described in the orthorhombic system. O are represented by dashed circles, Li by open circles, K by shaded circles and S by dotted circles.

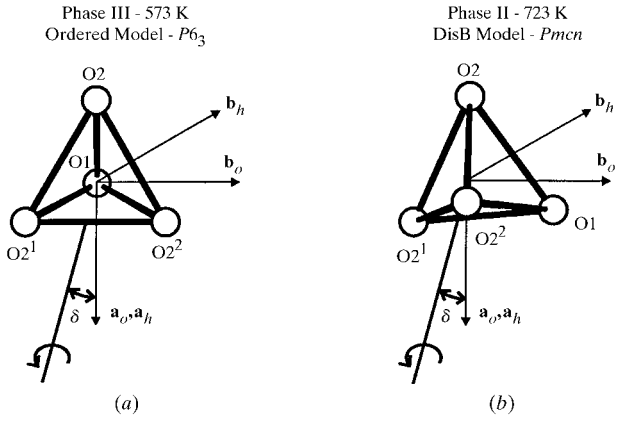

Figure 13
Rotation direction of the SO_4 group in the phase III ↔ II transition. h and o subscripts designate directions in the hexagonal and orthorhombic cells. The basal oxygen O2^{ii} [(ii) $-y, x - y, z$] in phase III (*a*) is transformed in the apical oxygen in phase II (*b*) by a rotation of the SO_4 unit around the indicated axis. Applying m_x in (*b*) one can generate the disordered structure observed in phase II. In order to better visualize the rotation direction $\delta = -4.5°$ is exaggerated here.

(trigonal distortion as seen in Fig. 3). This similarity can be explained by assuming the same type of disorder in both phases and that the split could not be properly evidenced in phase III.

The analyses of the data obtained at 723 and 803 K show no significant difference in the structure, except for the degree of disorder. The disordered model used in the description of phase I can be interpreted in terms of an increase in the tilting of the SO_4 groups observed on phase II; the equivalent but non-identical tetrahedra in phase II (*Pmcn* pseudo-hexagonal symmetry) would became identical after the transition leading to symmetry $P6_3/mmc$.

We would like to thank Professor Dieter Schwarzenbach and Henrik Birkedal (Lausanne, Switzerland), Dr Václav Petříček (Praha, Czech Republic), and Daniel R. Ventura (Vičosa, Brazil) for helpful discussions. This work was partially supported by CNPq (Conselho Nacional de Desenvolvimento Tecnológico, Brazil) and FAPEMIG (Fundação de Amparo a Pesquisa do Estado de Minas Gerais).

References

Bachmann, R. & Schulz, H. (1984). *Acta Cryst.* A**40**, 668–675.
Becker, P. J. & Coppens, P. (1974*a*). *Acta Cryst.* A**30**, 129–147.
Becker, P. J. & Coppens, P. (1974*b*). *Acta Cryst.* A**30**, 148–153.
Bhakay-Tamhane, S., Sequeira, A. & Chidambaram, R. (1984). *Acta Cryst.* C**40**, 1648–1651.
Borisov, B. F., Charnaya, E. V. & Radzhabov, A. K. (1994). *Phys. Status Solidus B*, **181**, 337–343.
Bradley, A. J. (1925). *Philos. Mag.* **49**, 1225–1237.
Chung, S. J. & Hahn, T. (1972). *Mater. Res. Bull.* **7**, 1209.
Chung, S. J. & Hahn, T. (1973). *Z. Kristallogr.* **137**, 447–449.
Flack, H. D. (1983). *Acta Cryst.* A**39**, 876–881.
Johnson, C. K. (1969/1970). *The Effect of Thermal Motion on Interatomic Distances and Angles*, Proc. Intl Summer School on Crystallographic Computing, Carleton University, Ottawa, Canada, August 1969; also in *Crystallographic Computing* (1970), edited by F. R. Ahmed, pp. 220–226. Copenhagen: Munksgaard.
Karppinen, M., Lundgren, J. O. & Liminga, R. (1983). *Acta Cryst.* C**39**, 34–38.
Klapper, H., Hahn, Th. & Chung, S. J. (1987). *Acta Cryst.* B**43**, 147–159.
Kuhs, W. F. (1988). *Aust. J. Phys.* **41**, 369–382.
Luk'yanchuk, I., Jório, A. & Pimenta, M. A. (1998). *Phys. Rev. B*, **57**, 5086–5092.
Li, Y. Y. (1984). *Solid State Commun.* **51**, 355–358.
Nacken, R. (1907). *Neues Jahrb. Mineral Beil.* **24**, 42–52.
Naruse, H., Tanaka, K., Morikawa, H. & Maruno, F. (1987). *Acta Cryst.* B**43**, 143–146.
Petříček, V. & Dušek, M. (1998). *JANA98 Crystallographic Computing System.* Institute of Physics, Academy of Sciences of Czech Republic.
Pietraszko, A. (1988). *Ferroelectrics*, **79**, 121–125.
Pimenta, M. A., Echegut, P., Luspin, Y., Hauret, G., Gervais, F. & Abelard, P. (1989). *Phys. Rev. B*, **39**, 3361–3368.
Sankaran, H., Sharma, S. M. & Sikka, S. K. (1988). *Solid State Commun.* **66–1**, 7–9.
Schefer, J., Schwarzenbach, D., Fischer, P., Koetzle, Th., Larsen, F. K., Haussühl, S., Rüdlinger, M., McIntyre, G., Birkedal, H. & Bürgi, H.-B. (1998). *Acta Cryst.* B**54**, 121–128.
Scherf, C., Hahn, T., Heger, G., Becker, R. A., Wunderlich, W. & Klapper, H. (1997). *Ferroelectrics*, **191**, 171–177.
Schulz, H., Zucker, U. & Frech, R. (1985). *Acta Cryst.* B**41**, 21–26.
Steurer, W., Wittmam, H., Jagodzinski, H. & Pietraszko, A. (1986). *Acta Cryst.* B**42**, 11–16.
Stoe & Cie (1996). *Stoe-IPDS® Software.* Stoe and Cie, Darmstadt GmbH, Germany.
Tanaka, K., Naruse, H., Morikawa, H. & Maruno, F. (1991). *Acta Cryst.* B**47**, 581–588.
Ventura, D. R., Speziali, N. L. & Pimenta, M. A. (1996). *Phys. Rev. B*, **54**, 11869–11872.
Welberry, T. R. & Glazer, A. M. (1994). *J. Appl. Cryst.* **27**, 733–741.
Willis, B. T. M. (1969). *Acta Cryst.* A**25**, 277–299.
Wyrouboff, G. (1890). *Bull. Soc. Fr. Mineral.* **13**, 215–233.
Zhang, M., Salje, E. K. N. & Putnis, A. (1998). *J. Phys.* **10**, 11811–11827.
Zhang, P. L., Yan, Q. W. & Boucherle, J. X. (1988). *Acta Cryst.* C**44**, 592–595.
Zucker, U. H. & Schulz, H. (1982*a*). *Acta Cryst.* A**38**, 563–568.
Zucker, U. H. & Schulz, H. (1982*b*). *Acta Cryst.* A**38**, 568–576.